Prey stoichiometry, primary production, and plankton composition influence production of marine crustacean zooplankton

Running head: Stoichiometry influences marine copepod production.

Pei-Chi Ho[1]: bookwormpageho@gmail.com

Esther Wong[2]: sonrysony@gmail.com

Fan-Sian Lin[1]: r01241202@ntu.edu.tw

Akash R. Sastri[3,4]: asastri@uvic.ca

Carmen García-Comas[5]: cgcomas@cmima.csic.es

Noboru Okuda[6]: nokuda@chikyu.ac.jp

Fuh-Kwo Shiah[7]: fkshiah@rcec.sinica.edu.tw

Gwo-Ching Gong[8,9]: gcgong@mail.ntou.edu.tw

Rita S.W. Yam[10]: ritayam@ntu.edu.tw

Chih-hao Hsieh[1, 7, 11, 12*]: chsieh@ntu.edu.tw

1. Institute of Oceanography, National Taiwan University, Taipei, Taiwan. 2. Division of Life Science, Hong Kong University of Science and Technology, Clear Water Bay, Hong Kong. 3. Department of Biology, University of Victoria, Victoria, BC, Canada. 4. Institute of Ocean Sciences, Fisheries and Oceans Canada, Sidney, BC, Canada. 5. Institute of Marine Sciences (ICM-CSIC), Barcelona, Spain 6. Research Institute for Humanity & Nature, Kyoto, Japan. 7. Research Center for Environmental Changes, Academia Sinica, Taipei, Taiwan. 8. Institute of Marine Environment and Ecology, National Taiwan Ocean University, Keelung, Taiwan. 9. Center of Excellence for the Oceans, National Taiwan Ocean University, Keelung, Taiwan. 10. Department of Bioenvironmental Systems Engineering, National

Taiwan University, Taipei, Taiwan. 11. Institute of Ecology and Evolutionary Biology, Department of Life Science, National Taiwan University, Taipei, Taiwan. 12. National Center for Theoretical Sciences, Taipei, Taiwan.

* Corresponding author: Chih-hao Hsieh. Full postal address: Institute of Oceanography, National Taiwan University, No. 1, Sec. 4, Roosevelt Rd., Taipei 10617, Taiwan.

Highlights:

- Subtropical marine copepod community production is low when prey molar C:N and C:P ratio is high.
- However, the variation of copepod production was large when prey C:N and C:P ratios were low.
- Multivariate regression indicates that prey C:N ratio explains the variation of copepod production most, followed by phytoplankton and copepod composition.
- Primary production exerts a weak influence on copepod production.

Abstract. Manipulative laboratory studies provide strong evidence that phytoplankton primary production (PP), stoichiometry and taxonomic composition affect marine copepod (biomass-dominant zooplankton group) production (CP). However, field observations investigating the simultaneous effects of prey stoichiometric quality, PP, and phytoplankton and copepod taxonomic composition on CP remain relatively scarce. Here, we examined how *in situ* CP is affected by carbon:nitrogen:phosphorus (C:N:P) molar ratios of prey, PP, and phytoplankton and copepod composition in the East China Sea (ECS) and Dongsha Atoll in the South China Sea. Field estimates of CP were measured directly as the product of *in situ* instantaneously growth rate estimates by artificial cohort method and copepod biomass. We found that CP was low when

prey C:N and C:P ratios were high (i.e. prey C exceeds copepod metabolic requirements), but the variation of CP was large when prey C:N and C:P ratios were low. CP did not, however, show a strong relationship with PP. Multivariate regression indicates that prey C:N ratio explains most of the variation of CP, followed by phytoplankton and copepod compositions, while PP exerts a weak influence on CP. Our findings suggest that copepod community production is affected by prey stoichiometry, with further modification by copepod and phytoplankton compositions in the ECS. However, the total variance explained by those key factors is less than 50 %, indicating that marine copepod growth and biomass production are influenced by complex factors in nature.

Keywords: Ecological stoichiometry; subtropical marine copepod production; artificial cohort method; *in situ* incubation; phytoplankton and copepod composition.

1. Introduction

Copepods represent the dominant zooplankton group and serve as an important trophic link between primary producers and higher trophic levels in the ocean (Alcaraz and Calbet, 2007). Identification of which factors influence copepod production (CP; mg C m^{-3} d^{-1}) is essential to understanding the dynamics of pelagic food webs in the oceans. Measuring egg production rate and biomass (assuming a constant growth rate) are two popular approaches used to assess CP in field studies (Castonguay et al., 2008; Hay et al., 1991; Hopcroft et al., 1998; Kiørboe and Nielsen, 1994; Mayor et al., 2009). However, neither egg production rate nor biomass fully represent CP and each prompts different ecological interpretation. Biomass production rates reflect the flux of carbon and energy from phytoplankton to copepods, which is viewed as the trophodynamic currency (Sheldon et al. 1977, Longhurst 1984). Egg production rates indeed reflect a part of CP, but this measurement does not include somatic growth during naupliar and copepodite stages (Hirst and McKinnon, 2001). The production of copepods may not be supported in the long term if egg production rate or biomass is high but somatic growth rates are slow. Thus, we need studies of *in situ* copepod community somatic growth-based production rate in order to better understand energy transferring in pelagic food webs.

Copepod growth and production rates can be limited by prey carbon supply, i.e., phytoplankton (Campbell et al., 2001; Hirst and Bunker, 2003). Thus, primary production (PP;

mg C m^{-3} d^{-1}) would be an important factor to support copepod production. However, copepod production is influenced not only by phytoplankton carbon supply, but also by the nitrogen content of phytoplankton (Kiørboe 2007). Thus, apart from carbon, stoichiometric constraints (the relative imbalance of elemental composition between consumers and prey) may limit copepod growth and production. Previous studies have indicated that crustacean consumers can grow efficiently only within an optimal range of prey stoichiometry (e.g. Laspoumaderes et al. 2015) and tend to be more stoichiometrically homeostatic than phytoplankton (Acharya et al., 2004; Sterner and Elser, 2002). The stoichiometric knife-edge hypothesis predicts that crustacean consumers must expend energy in order to respire and excrete assimilated elements in excess of their homeostatic demands (i.e. suboptimal prey C:N:P ratio; Boersma and Elser, 2006; Elser et al., 2016; Hessen et al., 2004). Occasionally, when phytoplankton C:N and C:P ratios are too low, crustacean consumers can be carbon-limited and must excrete the excess N and P; under this condition, crustacean growth also decreases.

Nitrogen (N) and phosphorus (P) play essential but distinct roles in animal growth and development (Elser et al., 2000). N is key to maintaining proteinaceous body structures, whereas P is essential to forming the rRNA backbone and thus controls protein synthesis and by extension, organism growth rate (Vrede et al., 2004). Given the physiological roles of both elements, low prey N and P contents lead to low rates of protein synthesis and rRNA production

for crustacean zooplankton and consequently hinder their biomass production and growth (Giani, 1991; Vrede et al., 2002). In addition, N- and P-deficiency of growth are not independent: under N-deficiency, the amounts of P and rRNA are decoupled from growth rate (Acharya et al., 2004). Thus, investigating the link between both N and P supplies versus copepod production provides a more detailed insight into CP variation. Considering the more strictly stoichiometric homeostasis of crustacean consumers, we expect that CP exhibits a unimodal pattern relative to prey C:N and C:P ratios.

In addition to the elemental stoichiometry of prey, the composition of biomolecules such as fatty acids (Müller-Navarra, 2008) may further constrain crustacean growth and development. Adding supplementary essential fatty acids or phytoplankton species with highly unsaturated fatty acids can improve crustacean growth (Brett and Müller-Navarra, 1997; Ferrão-Filho et al., 2003). Also, different copepod taxa and their life stages vary in growth strategy and responses to prey stoichiometry (Laspoumaderes et al., 2010; Villar-Argaiz et al., 2002), indicating that copepod taxonomic and stage composition may also influence CP. Thus, we should consider the effects of phytoplankton composition, copepod composition and copepod life stage structure on CP.

Understanding the link between CP versus PP, prey stoichiometry and composition in natural systems faces at least two challenges: First, estimation of *in situ* growth-based CP

requires intensive effort for onboard incubations and analyses (Runge and Roff, 2000); Second, a broad sampling area and/or time range should be covered to encompass sufficient light and trophic gradients (Finkel et al., 2006). Here, we addressed these challenges by applying the 'improved' artificial cohort method (Lin et al., 2013b) to measure copepod community growth and production rates in the East China Sea and around the Dongsha Atoll in the South China Sea. Both growth and production rate estimates were accompanied by measurements of prey stoichiometry, PP, and phytoplankton and copepod compositions. The large variation of nutrient supply and sea surface light intensity in the sampling areas ensured sufficient variation in PP, prey stoichiometry, and phytoplankton and copepod compositions for this study (Table A.1). Given the broad set of conditions, we were able to test the following hypotheses: (H1) CP decreases when prey molar C:N and C:P ratios are high (excessive C supply) or too low (excessive N and P supply) according to the stoichiometric knife-edge; (H2) CP increases with PP according to classical bottom-up effects; and (H3) phytoplankton and copepod compositions affect CP.

2. Materials and methods

2.1. Estimation of in situ copepod growth rate and production

We conducted 54 experiments during 2009-2016. The sampling cruises were mainly in the southern East China Sea, while cruises in the northern East Chinas Sea and around the Dongsha Atoll were also included (Fig. A.2, Table A.1). Growth (d^{-1}) and production (mg C m^{-3} d^{-1}) rates were estimated for copepod communities, which account for about 70% of the mesozooplankton biomass in the study area (Tseng et al., 2012). We applied the 'improved' artificial cohort method (see modifications to Kimmerer and Mckinnon 1987 by Lin et al. 2013b) to estimate the specific growth rate GR_i for each juvenile group; where, *i* corresponds to each of five copepodite groups (calanoid, cyclopoid, corycaeid, oncaeid, and harpacticoid copepodites) and three naupliar groups (calanoid, cyclopoid, and harpacticoid nauplii). We performed shipboard incubations of two size fractions, 50-80 μm (nauplius) and 100-150 μm (copepodite) copepods, in 3 replicates of 20-L collapsible polyethylene cubitainers. We collected the natural assemblage of phytoplankton smaller than 50 μm and excluded large phytoplankton for juvenile copepod incubation, considering that nauplii and copepodites of our target size range mainly feed on small prey of about 10 μm (an optimal length ratio of 18; Hansen et al. 1994). Seawater with phytoplankton at 10-m depth was collected using 20-L Go-Flo bottles, and screened it through 50-μm mesh prior to filling of cubitainers to ~90% capacity. Seawater accompanying the size-fractionated copepods made up the remaining volume of the 20-L cubitainers (Fig. A.1 in Appendix A).

We used two Norpac nets, a 50- and a 100-μm mesh to collect live animals (mainly copepods) for incubations of size-fractionated copepods. At each sampling site, the nets were set to 10-m depth and allowed to drift with the ship for 5−10 min. The contents of each net were carefully re-suspended in buckets filled with pre-screened incubation seawater. After gentle mixing, the contents of the 50-μm net were reverse-filtered through an 80-μm mesh and siphoned (~2 L) into cubitainers for the 50−80 μm artificial cohort incubations. Another subsample from the 80-μm mesh reverse filtrate was preserved in 5% formalin-buffered seawater to calculate the biomass distribution at the start of the incubation. The same process was applied to the contents of the 100-μm mesh net, but reverse-filtered with a 150-μm mesh, to establish the 100−150 μm artificial cohort. All cubitainers were incubated in 200-L dark black tanks filled with circulating seawater pumped constantly from the sea surface layer (Fig. A.1 in Appendix A).

We set the incubation time to 24 h for the 50−80 μm and 48 h for the 100−150 μm size fraction in order to ensure that growth was measurable (Lin et al., 2013a). The environment in the cubitainers was assumed to be similar to *in situ* conditions during the incubation, except that the tanks were always kept dark during incubation. Such a design aims to limit the growth of primary producers during incubation. At the end of shipboard experiments, we terminated the incubations and preserved the individuals in 5% formalin-buffered seawater (Lin et al., 2013a).

We estimated the body size distribution of copepodites and nauplii at the start and end of incubations. For samples collected early in the study period (29 samples), we used a dissecting microscope. We identified and enumerated copepod groups in the preserved samples (in total ~500 individuals), and took individual images with a CCD camera mounted on the microscope (Olympus DP71 with the software analySIS LS Starter 2.6). From these copepod digital images, we measured individual prosome length and width and calculated the biovolume of each individual nauplius and copepodite as: Biovolume (μm^3) = prosome length × width^2 (Lin et al., 2013a; Wong et al., 2017). For samples collected later (25 samples), we measured body size automatically with the FlowCAM. We set the FlowCAM to the 4X objective (effective magnification = 40X) and 300-μm flow cell (optimal for size range 30−300 μm) to capture the copepodite and naupliar images in autoimage mode. We then transformed the area-based diameter (ABD) biovolume to equivalent microscope-measured biovolume applying the equations reported by Wong et al. (2017). This transformation ensures that the growth rates estimated by the two methods are comparable in our study. We then calculated specific growth rates (d^{-1}) of all juvenile groups based on the assumption of exponential growth (Lin et al., 2013a) as follows: $GR_i = \ln(W_{iT} / W_{i0}) / T$, where W_{i0} and W_{iT} are the modes of biovolume (μm^3) at the start and end of incubation, respectively, and T is the incubation time: 1 day (24 hours) for the 50−80 μm and 2 days (48 hours) for the 100−150 μm size fraction (Lin et al. 2013b).

Some issues and caveats associated with our *in situ* artificial cohort incubations and efforts to account for and minimize them are worth discussion. We selected specific size ranges (50-80 and 100-150 μm) to represent the nauplius and copepodite cohorts by reverse filtration (McKinnon and Duggan, 2003; Runge and Roff, 2000), but some adult individuals might still leak into the incubation; we have excluded these adult individuals when classifying and measuring juvenile body sizes to avoid bias. Furthermore, using peak instead of mean body size, we were able to avoid the influence of extreme body sizes in the cohort (Lin et al., 2013b). One potential source of bias that we were not able to quantify is mortality during incubations. In addition to mortality, competition among copepods and other zooplankton may also influence the growth rate, though the low density of non-copepod species and sufficient food and space conditions in the cubitainers should serve to reduce this effect.

To eliminate effects of temperature on growth, we standardized all the GR_i to 20 °C through the Van't Hoff-Arrhenius equation (Brown et al., 2004). To calculate copepod community production rates, we measured the biomass (B_i) of each copepod group. To obtain group-specific biomass, we collected copepodites and nauplii with a 50 μm mesh Norpac net equipped with a mechanical flow meter (HYDRO-BIOS) and preserved the samples in seawater-buffered 10 % formalin. We sorted and counted the number of individuals for each group. Volumes filtered by the nets were estimated from the flow meter and applied group-specific abundances to calculate

density (ind m^{-3}). Densities were then multiplied by mean C biomass for each group. The mean C body mass of each copepod group was calculated from the individual biovolume distribution at the start of each incubation. Copepod biovolume was transformed to wet weight (WW) following Svetlichny (1983): WW = Kc × Biovolume, where Kc is 0.6 for calanoids and 0.705 for cyclopoids (see McKinnon and Duggan 2003), and 0.65 for groups where conversion factors were not available. The wet weight was then transformed to C body mass (CB) by dry weight (DW) = 0.135×WW (Postel et al., 2000) and CB = 0.42 × DW (Beers, 1966). Assuming exponential growth, the daily group-specific biomass increment of group-specific production $\mathrm{CP}_i = B_i(e^{\mathrm{GR}_i} - 1)$ and community $\mathrm{CP} = \sum_i \mathrm{CP}_i$.

3.2. Prey stoichiometry, biomass and PP measurements

As a proxy for prey (mainly phytoplankton) stoichiometry, we measured the C:N:P molar ratio of particulate organic matter (POM) from the euphotic zone, where photosynthesis and grazing are focused. We collected POM < 50 μm from 50-μm sieve-filtered water samples (5 L water was filtered from 20 L Go-Flo bottles each depth; sampling 4 depths in the euphotic zone) onto pre-combusted GF/F papers (500°C, 6 hours), and froze the POM samples at −20 °C on board. Prior to elemental analysis, samples were acidified and dried for at least 24 hours to remove inorganic carbon. We used an elemental analyzer (EA1108, Fisons, Italy, and FLASH

2000, Thermo SCIENTIFIC, USA) to measure the C and N content in the POM. The P content was measured using molybdate spectrophotometric analysis following wet digestion of POM samples with nitric acid (Parsons et al., 1984). The P content in 17 of the 54 samples was below detection limit. The prey C:N:P molar ratios were then calculated from the C, N, and P contents in POM. Finally, PP (mg C m^{-3} d^{-1}) was estimated with an on-board carbon radioisotope incubation method (Gong and Liu, 2003).

3.3. Assessing phytoplankton and copepod compositions

In addition to prey stoichiometry and PP, we also considered the taxonomic/group compositions of copepods and phytoplankton as potential factors affecting CP. Phytoplankton composition (biovolume composition of morphological groups) from the euphotic zone was enumerated for only 34 of the 54 experiments. We used the biovolume composition of phytoplankton considering that phytoplankton biomass, instead of abundance, limits zooplankton growth. The relative biovolume of phytoplankton group *i* was calculated as:

$$R_{iB} = \frac{\sum_{m} \mathrm{BioV}_{i,m}}{\sum_{j \neq \mathrm{detritus}} \sum_{n} \mathrm{BioV}_{j,n}},$$

where $\mathrm{BioV}_{i,m}$ is the ESD biovolume (μm^3) of cell *m* classified as group *i* (small phytoplankton, medium phytoplankton, large phytoplankton, diatoms, dinoflagellates, ciliates, and cyanobacteria;

see Appendix C), and the denominator is the total phytoplankton biovolume excluding detritus. The copepod composition was calculated for all incubations. Here, we focused on abundance composition of the copepod juvenile groups included in the artificial cohort experiment, given that the interactions between copepod juveniles are at the individual level. The abundance ratio of copepod group *i* (copepodites of calanoid, cyclopoid, corycaeid, oncaeid, harpacticoid, and nauplii; see Appendix C) was calculated as $R_{i\#} = n_i \Big/ \sum_j n_j$, where n_i is the abundance (ind m^{-3}) of group *i* and the denominator is the sum of all copepod group abundances. See Apppendix C for detailed descriptions of phytoplankton and copepod grouping procedures.

3.4. Statistical analysis

To test if CP decreases with high and/or excessively low prey C:N and C:P ratios (H1), we first plotted CP against prey C:N or C:P ratio. Visually, we saw no evidence of low CP under low prey C:N or C:P ratio, rather we observed a declining trend (Fig. 1). Thus, we applied linear regressions of CP versus prey elemental ratios. To test if CP increases with PP (H2), we applied linear regression of CP versus PP. The regression relationships were estimated with the *lm* functions of the R package *stats*. We also depicted PP by color on the CP versus C:N (C:P) ratio scatter plot, and C:N ratio on the CP versus PP scatter plot to visualize the additive effects of prey stoichiometry and PP on CP (see Fig. 1). We further applied quantile regressions (*rq*

function in R package *quantreg*) to investigate the relationships between CP versus prey stoichiometry and PP under different levels of CP (Fig. B.1).

In addition, we employed multivariate linear regression to investigate the relative effects of prey stoichiometry, PP, phytoplankton and copepod compositions on CP (H3). The relative C biomass of dominant phytoplankton groups ($R_{MediumB}$ and R_{LargeB} as medium and large phytoplankton ratios, $R_{DiatomB}$ as diatom ratio) and dinoflagellates (R_{DinoB}) that occasionally bloom (Fig. C.1a in Appendix C), and relative abundance of the dominant copepodite groups ($R_{Cal\#}$ and $R_{Cyc\#}$ as calanoid and cyclopoid ratios) and nauplii ($R_{Nau\#}$) (Fig. C.1b in Appendix C) were incorporated into the full model of multivariate regression (see details in Appendix C). We identified the most parsimonious model on the basis of Akaike's information criterion (AIC) following a stepwise model selection using the *stepAIC* function of the R package *MASS*. Furthermore, the relative importance of these variables on CP in the most parsimonious model was assessed by their R^2 contribution using the R package *relaimpo*.

4. Results

4.1. Does CP decrease with suboptimal prey C:N and C:P ratios (H1)?

Linear regression analyses indicates a statistically significant decline of CP with prey C:N ratio (Fig. 1a; CP = −0.088 Prey C:N+0.768, $R^2 = 0.190$, $p = 0.001$, $n = 54$), but the linear

regression of CP versus prey C:P ratio was not significant (Fig. 1b; CP = -9.852×10^{-5} Prey C:P + 0.290, $R^2 = 0.042$, $p = 0.224$, $n = 37$). The quantile regressions exhibited that only the quantiles ≥ 50 % showed significantly negative relationships between CP and prey C:N (50% and 90% quantiles) and between CP and prey C:P (75% quantile) (Fig. B.1a and b).

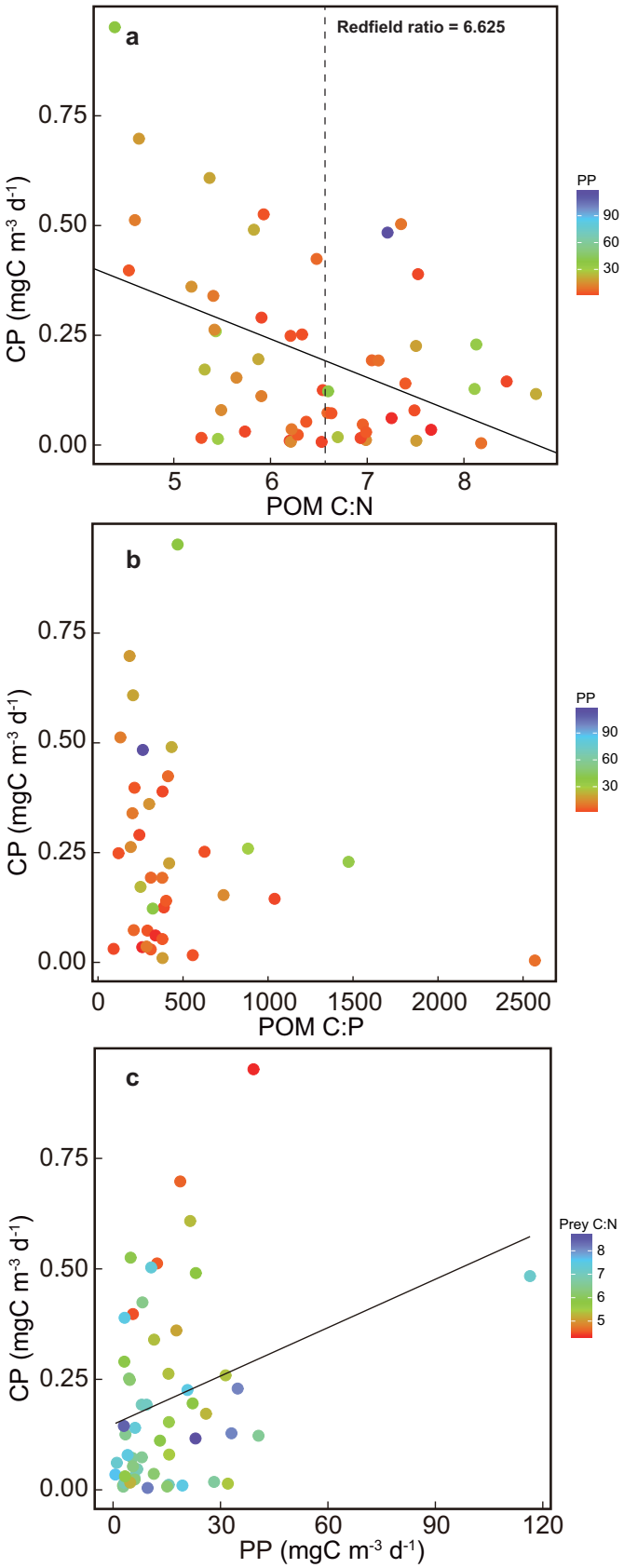

Figure 1. Relationship between copepod production (CP) versus (a) POM C:N ratio, (b) POM

C:P ratio and (c) PP. The vertical dashed line indicates the Redfield ratio in (a). The color of the symbols in (a) and (b) represents PP (mg C m^{-3} d^{-1}). The vertical dashed line in (a) indicates the Redfield molar C:N ratio. The color of the symbols in (c) represents POM C:N ratio (mole:mole). The solid ($p < 0.05$) lines represent the results of linear regression.

4.2. Does CP increase with high PP (H2)?

PP could be a determinant factor influencing CP (Fig 1c; CP = 0.004 PP + 0.148, $R^2 = 0.095$, $p = 0.024$, $n = 54$); however, the regression becomes non-significant (CP = 0.005 PP + 0.129, $R^2 = 0.072$, $p = 0.052$, $n = 53$) after removing an extremely high PP outlier value (> 100 mg C $m^{-3}d^{-1}$). Moreover, the quantile regressions were not significant for any quantile (Fig. B.1c).

4.3. Is CP influenced by copepod and phytoplankton compositions (H3)?

Along with prey C:N ratio (the main stoichiometric ratio that influences CP) and PP, we incorporated the relative biomass of dominant phytoplankton groups, and the relative abundance of the dominant nauplii and copepodite groups into the multivariate model (Appendix C). The most parsimonious model explaining variation in the CP includes: prey molar C:N ratio (Prey C:N), cyclopoid copepodite abundance ratio ($R_{Cyc\#}$), and dinoflagellate biomass ratio (R_{DinoB}) (Table 1; the best multivariate linear model: CP = −0.182 Prey C:N – 1.092 $R_{Cyc\#}$ + 0.602 R_{DinoB}

+ 1.385, $R^2 = 0.418$, $p = 0.001$, $n = 34$). The relative importance of the three variables follows the order: Prey C:N > $R_{Cyc\#}$ > R_{DinoB} (Table 2).

Initial model: CP = Prey C:N + PP + $R_{MediumB}$ + R_{LargeB} + $R_{DiatomB}$ + R_{DinoB} + $R_{Cal\#}$ + $R_{Cyc\#}$ + $R_{Nau\#}$	
Step	AIC
	−95.37
− PP	−97.35
− $R_{DiatomB}$	−99.20
− $R_{MediumB}$	−100.94
− R_{LargeB}	−102.66
− $R_{Nau\#}$	−102.83
− $R_{Cal\#}$	−103.45
Most parsimonious model: CP = 1.385 − 0.182 Prey C:N + 0.602 R_{DinoB} − 1.092 $R_{Cyc\#}$	

Table 1. AICs of multivariate linear regressions and stepwise model selection for investigating the factors that determine copepod production (CP). $R_{MediumB}$, R_{LargeB}, $R_{DiatomB}$ and R_{DinoB} represents the biomass ratios of medium, large phytoplankton, diatoms, and dinoflagellates to total phytoplankton biomass. $R_{Cal\#}$, $R_{Cyc\#}$, and $R_{Nau\#}$ represents the abundance ratio of calanoid copepodites, cyclopoid copepodites, and all nauplii to total copepod abundance. There are 34 sets of experiments with complete CP, stoichiometry, PP, and plankton composition data.

Variable	Relative importance
Prey C:N	0.762
$R_{Cyc\#}$	0.191
R_{DinoB}	0.047

Table 2. Relative contributions of variables explaining the variation of copepod production (CP) in the most parsimonious model.

5. Discussion

5.1. Prey stoichiometry, especially prey C:N ratio, affects CP

CP is lower when prey molar C:N and C:P ratios are high (Fig. 1a and C:P ratio > 500 in Fig. 1b), inferring that low N and P in food may limit CP. It is worth noting that we found a clearer reduction of CP with high prey C:N than with high C:P ratio, which infers that N limitation seems to be more important to copepod community production rate in our studied marine areas. The biomass of copepods also decreased significantly with increasing prey C:N ratio, showing a similar trend to CP with prey C:N ratio (Fig. 2; Copepod biomass = −0.511 Prey C:N + 4.723, R^2 = 0.085, p = 0.032, n = 54). This may be due to our focus on marine copepods, which are more sensitive to N limitation than cladocerans (Hassett et al., 1997; Sterner and Elser, 2002). Furthermore, CP and copepod biomass were dominated by copepodites (Fig. B.3 and B.4), which

have higher N demand than nauplii (that is, copepodites have significantly lower C:N and slightly higher N:P ratio than nauplii, Fig. B.2a and c in Appendix B; also see Villar-Argaiz et al. 2002 and Meunier et al. 2015). Though naupliar abundance is high in tropical copepod communities, naupliar biomass and production rates are usually much lower compared with copepodites, due to the low body mass of nauplii (Hopcroft et al., 1998). Thus, prey N-deficiency that decreases copepodite growth should affect copepod community production more strongly.

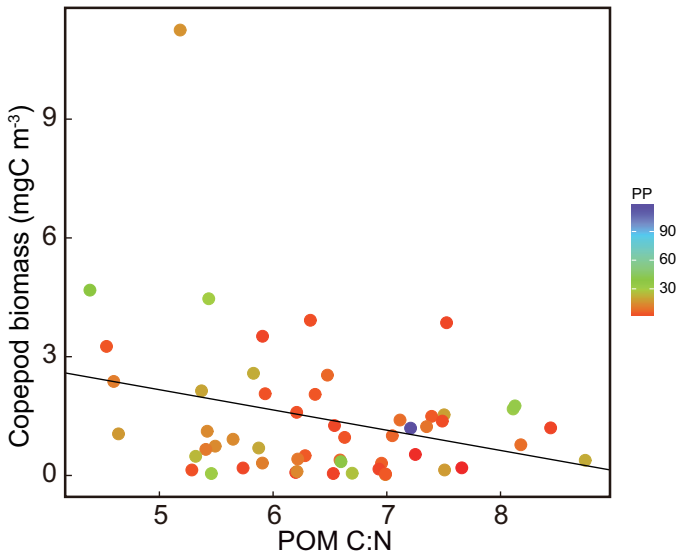

Figure 2. Relationship between copepod community carbon biomass versus POM C:N ratio. The color of the symbols represents PP (mg C m^{-3} d^{-1}). The solid ($p < 0.05$) line represents the result of linear regression.

We found that low CP is associated with high prey C:N ratio, suggesting that copepod carbon biomass production is more limited by N, rather than C, in our study area. However, we found large variation of CP when the C:N ratio of prey is below or approximately the same as that of copepods (below Redfield ratio 6.625 in Fig. 1a; Gismervik 1997). This contradicts to the knife-edge hypothesis that CP should decrease when prey nitrogen is in excess. To find out what may explain the high variation of CP when the prey molar C:N ratio is below Redfield (< 6.625), we applied stepwise multiple linear regression to explain CP considering the relative abundance of copepod groups. We found that the model includes only the naupliar abundance ratio (considering only data of prey C:N ratio < 6.625: $CP = 0.579\ R_{Nau\#} - 0.110$, $R^2 = 0.130$, $p = 0.043$, $n = 32$; Table 3), suggesting that dominance of nauplii increases CP when prey N is higher than the need of copepods. That is, when naupliar and copepodite growth is not nitrogen-limited, the higher abundance of fast-growing early life stages (i.e. nauplii) would increase the total biomass production of the copepod community (Hopcroft et al., 1998; Hopcroft and Roff, 1998; Hygum et al., 2000; Leandro et al., 2006).

Initial model: $CP = R_{Cal\#} + R_{Cyc\#} + R_{Nau\#}$	
Step	AIC
	−68.52
$- R_{Cal\#}$	−69.22
$- R_{Cyc\#}$	−70.56
Most parsimonious model: $CP = 0.579\ R_{Nau\#} - 0.110$	

Table 3. AICs of multivariate linear regressions and stepwise model selection for investigating the factors that determine copepod production (CP) when POM C:N < 6.625 (Redfield ratio). $R_{Cal\#}$, $R_{Cyc\#}$, $R_{Nau\#}$ represents the abundance ratio of calanoid copepodites, cyclopoid copepodites, and all nauplii to total copepod abundance. There are 32 sets of experiments with POM molar C:N < 6.625, CP, and plankton composition data.

5.2. Primary production influences CP, but is not the main limiting factor for CP

The classical bottom-up effect was observed in the East China Sea and the Dongsha Atoll, but did not affect CP as strongly as the prey C:N ratio (Fig. 1c). We found that the most parsimonious multivariate regression model does not include PP; that is, PP may not be the most important factor explaining CP (Table 1). In particular, at low PP (PP < 30 mg C m^{-3} d^{-1}), we found that high CP occurred with lower prey C:N ratios (Fig. 1c). This indicates that low PP may still support appreciable CP when prey nitrogen content is sufficient. Whereas previous studies reported an interactive influence of phytoplankton P content and PP on the production of

freshwater herbivores (Persson et al., 2007; Urabe et al., 2002), we found that sufficient prey N is related to high CP in this subtropical marine system.

5.3. Prey and copepod compositions affect CP

While prey C:N ratio has the highest relative importance in the multivariate model, the abundance ratio of cyclopoid copepodites and the biomass ratio of dinoflagellates also makes significantly contributions to variation of CP (Table 1 and Table 2). The negative relationship between CP and cyclopoid copepodites may be due to the lower growth rates of cyclopoid relative to calanoid copepodites (Hirst and Lampitt, 1998; Lin et al., 2013a). The positive correlation between CP and the dinoflagellate biomass ratio has been supported by diet manipulation experiments, where copepods consuming a mixture of dinoflagellates and microzooplankton grow better than feeding on a diatom-dominant diet (Nejstgaard et al., 2001). We infer from this result that prey and copepod compositions potentially influences the trophic interactions and CP, as proposed in our third hypothesis. In this study, we have focused on investigating total CP. Whereas, contrasting the difference in production among copepod taxonomic groups and stages could be interesting. These taxonomy- and stage-specific analyses will be reported in a separate work.

5.4. Other trophic interactions and environmental conditions that may determine CP

Though we found that CP decreases with high prey C:N ratios and that it is additionally affected by both prey and copepod composition, these three factors together explain less than half the variation of CP (R^2 = 0.418). The quantile regressions also showed that only the regressions of quantiles ≥ 50 % are significant (Fig. B.1a; regressions are significant at quantiles 90% and 50%), indicating that stoichiometry alone could not explain those observations of low CP well. The other source of CP variation may be due to the reaction time needed for prey stoichiometry to change. The study of Malzahn and Boersma (2012) found that exposure to P-limiting food cause long-lasting reduction of copepod growth even after re-feeding with a P-sufficient prey. However, the C:N and C:P ratio of POM we measured is a snapshot of prey stoichiometry at the start of our incubations and does not necessarily reflect what the copepods experienced before incubation. Thus, if copepod growth has not adapted to change of prey stoichiometry, we may see a mismatch of observed prey stoichiometry and CP.

We also noted some caveats associated with our measurements of prey C:N and C:P ratio: POM ≤ 50 μm includes phytoplankton as well as microzooplankton, mixotrophic protists (Flynn et al., 2013), and detritus (non-living particles; Postel et al. 2000). Microzooplankton and mixotrophic protists are key organisms in microbial food webs (Azam et al., 1983) and influence energy transfer to mesozooplankton (Calbet and Saiz, 2005), but we did not investigate the effect

of the microbial food web in this study. Furthermore, the existence of C-rich detritus (dead biomass) in the POM may increase the C:N or C:P ratio that we observed. Nevertheless, copepods can selectively choose living cells which have lower C:N and C:P ratios instead of ingesting dead biomass (Demott, 1988; Paffenhöfer and Sant, 1985), suggesting that the realized prey C:N and C:P ratios consumed by copepods may be lower than the POM C:N and C:P ratio we measured. With our current data, we could not separate the stoichiometric contribution of phytoplankton, microzooplankton and detritus to POM, and thus in this study we are not able to investigate these hidden trophic interactions.

6. Conclusions

In summary, our study demonstrates that copepod biomass production is mainly limited by prey stoichiometry in the subtropical marine ecosystems. In particular, when prey molar C:N or C:P ratio is high, CP is low. However, when prey molar C:N or C:P ratio is low, CP variation is large, highlighting the complexity of understanding CP in natural systems. Furthermore, copepod and phytoplankton compositions influence copepod community production as well. Interestingly, PP explained only a minor portion of the variation in copepod community production in the East China Sea and South China Sea. In conclusion, our *in situ* incubation experiments highlight the knowledge gained by measuring copepod growth and production rates for understanding

stoichiometric effects on copepod community, and also apprehend the complexity of copepod production variation in nature.

Authors' contributions

C-H. H. and P-C. H. conceived the research question. E. W., A. S., P-C. H. and F-S. L. operated *in situ* incubation experiments and measured copepod size distribution. P-C. H. and N. O. measured the C and N contents of POM and zooplankton. P-C. H. and R. S. W. Y. designed the procedures and measured the P contents of POM and zooplankton. C-H. H., P-C. H., E. W., and F-S. L. collected POM and zooplankton samples. G-C. G. and F-K. S. measured PP and environmental data. F-S. L. and C. G-C. measured the composition of the phytoplankton. P-C. H. analyzed the data. P-C. H. wrote the manuscript and all authors contributed to the revision.

Acknowledgements

We thank the crew of Ocean Researcher I and II for sampling. We thank Yu-Ching Lee, Yu-Chu Lin, Guo-Sheng Lyu and Tz-Chian Chen for carrying out FlowCAM analyses and classifying copepod images. This work was supported by the National Center for Theoretical Sciences, Foundation for the Advancement of Outstanding Scholarship, and the Ministry of Science and Technology, Taiwan. The Cooperative Research Facilities of the Center for

Ecological Research, Kyoto University, was partly used for the elemental analysis.

Declarations of interest: none.

Statement for data archiving

We agree to make the data necessary to reproducing our results available on Dryad Digital Repository and R codes for analysis on GitHub.

References

Acharya, K., Kyle, M., Elser, J.J., 2004. Biological stoichiometry of *Daphnia* growth: An ecophysiological test of the growth rate hypothesis. Limnol. Oceanogr. 49, 656–665.

Alcaraz, M., Calbet, A., 2007. Large zooplankton: its role in pelagic food webs, in: Safran, P. (Ed.), Fisheries and Aquaculture. Eolss Publishers, pp. 243–265.

Azam, F., Fenchel, T., Field, J.G., Meyer-Reil, L.A., Thingstad, F., 1983. The ecological role of water-column microbes in the sea. Mar. Ecol. Prog. Ser. 10, 257–283.

Beers, J.R., 1966. Studies on the chemical composition of the major zooplankton groups in the Sargasso Sea off Bermuda. Limnol. Oceanogr. 11, 520–528. https://doi.org/10.4319/lo.1966.11.4.0520

Boersma, M., Elser, J.J., 2006. Too much of a good thing : on stoichiometrically balanced diets and maximal growth. Ecology 87, 1325–1330.

Brett, M.T., Müller-Navarra, D.C., 1997. The role of highly unsaturated fatty acids in aquatic food web processes. Freshw. Biol. 38, 483–499. https://doi.org/10.1046/j.1365-2427.1997.00220.x

Brown, J.H., Gillooly, J.F., Allen, A.P., Savage, V.M., West, G.B., 2004. Toward a metabolic theory of ecology. Ecology 85, 1771–1789.

Calbet, A., Saiz, E., 2005. The ciliate-copepod link in marine ecosystems. Aquat. Microb. Ecol. 38, 157–167.

Campbell, R.G., Wagner, M.M., Teegarden, G.J., Boudreau, C.A., Durbin, E.G., 2001. Growth and development rates of the copepod *Calanus finmarchicus* reared in the laboratory. Mar. Ecol. Prog. Ser. 221, 161–183.

Castonguay, M., Plourde, S., Robert, D., Runge, J.A., Fortier, L., 2008. Copepod production drives recruitment in a marine fish. Can. J. Fish. Aquat. Sci. 65, 1528–1531. https://doi.org/10.1139/F08-126

Demott, W.R., 1988. Discrimination between algae and detritus by freshwater and marine zooplankton. Bull. Mar. Sci. 43, 486–499.

Elser, J.J., Kyle, M., Learned, J., McCrackin, M.L., Peace, A., Steger, L., 2016. Life on the

stoichiometric knife-edge : effects of high and low food C:P ratio on growth, feeding, and respiration in three *Daphnia* species. Inl. Waters 6, 136–146. https://doi.org/10.5268/IW-6.2.908

Elser, J.J., Sterner, R.W., Gorokhova, E., Fagan, W.F., Markow, T.A., Cotner, J.B., Harrison, J.F., Hobbie, S.E., Odell, G.M., Weider, L.J., 2000. Biological stoichiometry from genes to ecosystems. Ecol. Lett. 3, 540–550.

Ferrão-Filho, A.S., Fileto, C., Lopes, N.P., Arcifa, M.S., 2003. Effects of essential fatty acids and N and P-limited algae on the growth rate of tropical cladocerans. Freshw. Biol. 48, 759–767.

Finkel, Z. V, Quigg, A., Raven, J.A., Schofield, O.E., 2006. Irradiance and the elemental stoichiometry of marine phytoplankton. Limnol. Oceanogr. 51, 2690–2701.

Flynn, K.J., Stoecker, D.K., Mitra, A., Raven, J.A., Glibert, P.M., Hansen, P.J., Granéli, E., Burkholder, J.M., 2013. Misuse of the phytoplankton – zooplankton dichotomy: the need to assign organisms as mixotrophs within plankton functional types. J. Plankton Res. 35, 3–11. https://doi.org/10.1093/plankt/fbs062

Giani, A., 1991. Implications of phytoplankton chemical composition for zooplankton production: experimental evidence. Oecologia 87, 409–416. https://doi.org/10.1007/BF00634599

Gismervik, I., 1997. Stoichiometry of some marine planktonic crustaceans. J. Plankton Res. 19, 279–285. https://doi.org/10.1093/plankt/19.2.279

Gong, G.-C., Liu, G.-J., 2003. An empirical primary production model for the East China Sea. Cont. Shelf Res. 23, 213–224. https://doi.org/http://dx.doi.org/10.1016/S0278-4343(02)00166-8

Hansen, B., Bjørnsen, P.K., Hansen, P.J., 1994. The size ratio between planktonic predators and their prey. Limnol. Oceanogr. 39, 395–403.

Hassett, R.P., Cardinale, B., Stabler, L.B., Elser, J.J., 1997. Ecological stoichiometry of N and P in pelagic ecosystems: Comparison of lakes and oceans with emphasis on the zooplankton-phytoplankton interaction. Limnol. Oceanogr. 42, 648–662.

Hay, S.J., Kiørboe, T., Matthews, A., 1991. Zooplankton biomass and production in the North Sea during the Autumn Circulation experiment, October 1987-March 1988. Cont. Shelf Res. 11, 1453–1476. https://doi.org/10.1016/0278-4343(91)90021-W

Hessen, D.O., Ågren, G.I., Anderson, T.R., Elser, J.J., Ruiter, P.C. de, 2004. Carbon sequestration in ecosystems : the role of stoichiometry. Ecology 85, 1179–1192.

Hirst, A.G., Bunker, A.J., 2003. Growth of marine planktonic copepods: global rates and patterns in relation to chlorophyll *a*, temperature, and body weight. Limnol. Oceanogr. 48, 1988–2010.

Hirst, A.G., Lampitt, R.S., 1998. Towards a global model of *in situ* weight-specific growth in marine planktonic copepods. Mar. Biol. 132, 247–257.

Hirst, A.G., McKinnon, A.D., 2001. Does egg production represent adult female copepod growth? A call to account for body weight changes. Mar. Ecol. Prog. Ser. 223, 179–199. https://doi.org/10.3354/meps223179

Hopcroft, R.R., Roff, J.C., 1998. Zooplankton growth rates : the influence of size in nauplii of tropical marine copepods. Mar. Biol. 132, 87–96.

Hopcroft, R.R., Roff, J.C., Lombard, D., 1998. Production of tropical copepods in Kingston Harbour, Jamaica : the importance of small species. Mar. Biol. 130, 593–604.

Hygum, B.H., Rey, C., B. W. Hansen, 2000. Growth and development rates of *Calanus finmarchicus* nauplii during a diatom spring bloom. Mar. Biol. 136, 1075–1085.

Kimmerer, W.J., Mckinnon, A.D., 1987. Growth, mortality, and secondary production of the copepod *Acartia tranteri* in Westernport Bay, Australia. Limnol. Oceanogr. 32, 14–28. https://doi.org/10.4319/lo.1987.32.1.0014

Kiørboe, T., 2007. Phytoplankton growth rate and nitrogen content: implications for feeding and fecundity in a herbivorous copepod. Mar. Ecol. Prog. Ser. 55, 229–234. https://doi.org/10.3354/meps055229

Kiørboe, T., Nielsen, T.G., 1994. Regulation of zooplankton biomass and production coastal

ecosystem . 1 . Copepods. Limnol. Oceanogr. 39, 493–507.

Laspoumaderes, C., Modenutti, B., Balseiro, E., 2010. Herbivory versus omnivory: linking homeostasis and elemental imbalance in copepod development. J. Plankton Res. 32, 1573–1582. https://doi.org/10.1093/plankt/fbq077

Laspoumaderes, C., Modenutti, B., Elser, J.J., Balseiro, E., 2015. Does the stoichiometric carbon:phosphorus knife edge apply for predaceous copepods? Oecologia 178, 557–569. https://doi.org/10.1007/s00442-014-3155-8

Leandro, S.M., Tiselius, P., Queiroga, H., 2006. Growth and development of nauplii and copepodites of the estuarine copepod *Acartia tonsa* from southern Europe (Ria de Aveiro, Portugal) under saturating food conditions. Mar. Biol. 150, 121–129. https://doi.org/10.1007/s00227-006-0336-y

Lin, K.-Y., Akash R. Sastri, Guo-Ching Gong, Hsieh, C., 2013a. Copepod community growth rates in relation to body size, temperature, and food availability in the East China Sea: a test of metabolic theory of ecology. Biogeosciences 10, 1877–1892.

Lin, K.-Y., Sastri, A.R., Hsieh, C., 2013b. An alternative kernel-based method for estimating copepod growth rates from multimodal biomass distributions in artificial cohort experiments. Zool. Stud. 52, 1–9.

Longhurst, A., 1984. Importance of measuring rates and fluxes in marine ecosystems, in: Fasham,

M.J.R. (Ed.), Flows of energy and materials in marine ecosystems: theory and practice. Springer US, Boston, MA, pp. 3–22. https://doi.org/10.1007/978-1-4757-0387-0_1

Malzahn, A.M., Boersma, M., 2012. Effects of poor food quality on copepod growth are dose dependent and non-reversible. Oikos 121, 1408–1416. https://doi.org/10.1111/j.1600-0706.2011.20186.x

Mayor, D.J., Anderson, T.R., Pond, D.W., Irigoien, X., 2009. Limitation of egg production in *Calanus finmarchicus* in the field: A stoichiometric analysis. J. Mar. Syst. 78, 511–517. https://doi.org/10.1016/j.jmarsys.2008.12.020

McKinnon, A.D., Duggan, S., 2003. Summer copepod production in subtropical waters adjacent to Australia's North West Cape. Mar. Biol. 143, 897–907. https://doi.org/http://dx.doi.org/10.1007/s00227-003-1153-1

Meunier, C.L., Boersma, M., Wiltshire, K.H., Malzahn, A.M., 2016. Zooplankton eat what they need: copepod selective feeding and potential consequences for marine systems. Oikos 125, 50-58. https://doi.org/10.1111/oik.02072

Müller-Navarra, D.C., 2008. Food web paradigms: the biochemical view on trophic interactions. Int. Rev. Hydrobiol. 93, 489–505. https://doi.org/10.1002/iroh.200711046

Nejstgaard, J.C., Hygum, B.H., Naustvoll, L.J., Båmstedt, U., 2001. Zooplankton growth, diet and reproductive success compared in simultaneous diatom- and flagellate-

microzooplankton-dominated plankton blooms. Mar. Ecol. Prog. Ser. 221, 77–91. https://doi.org/10.3354/meps221077

Paffenhöfer, G.-A., Sant, K.B. Van, 1985. The feeding response of a marine planktonic copepod to quantity and quality of particles. Mar. Ecol. Prog. Ser. 27, 55–65. https://doi.org/10.3354/meps027055

Parsons, T.R., Maita, Y., Lalli, C.M., 1984. A manual of chemical and biological methods for seawater analysis. Pergamon Press.

Persson, J., Brett, M.T., Vrede, T., Ravet, J.L., 2007. Food quantity and quality regulation of trophic transfer between primary producers and a keystone grazer (*Daphnia*) in pelagic freshwater food webs. Oikos 116, 1152–1163. https://doi.org/10.1111/j.2007.0030-1299.15639.x

Postel, L., Fock, H., Hagen, W., 2000. 4 Biomass and abundance, in: Harris, R., Wiebe, P., Lenz, J., Skjoldal, H.R., Huntley, M. (Eds.), ICES zooplankton methodology manual. Academic Press, pp. 83–174. https://doi.org/10.13140/2.1.4985.3765

Runge, J.A., Roff, J.C., 2000. 9 The measurement of growth and reproductive rates, in: Harris, R., Wiebe, P., Lenz, J., Skjoldal, H.R., Huntley, M. (Eds.), ICES zooplankton methodology manual. Academic Press, pp. 401–454.

Sheldon, R.W., Sutcliffe Jr., W.H., Paranjape, M. a., 1977. Structure of pelagic food chain and

relationship between plankton and fish production. J. Fish. Res. Board Canada 34, 2344–2353. https://doi.org/10.1139/f77-314

Sterner, R.W., Elser, J.J., 2002. Ecological stoichiometry : the biology of elements from molecules to the biosphere. Princeton University Press, Princeton, NJ.

Svetlichny, L., 1983. Calculation of planktonic copepod biomass by means of coefficients of proportionality between volume and linear dimensions of the body. Ecol. Morja 15, 46–58.

Tseng, L.-C., Dahms, H.-U., Chen, Q.-C., Hwang, J.-S., 2012. Mesozooplankton and copepod community structures in the southern East China Sea : the status during the monsoonal transition period in September. Helgol. Mar. Res. 66, 621–634. https://doi.org/10.1007/s10152-012-0296-1

Urabe, J., Kyle, M., Makino, W., Yoshida, T., Andersen, T., Elser, J.J., 2002. Reduced light increases herbivore production due to stoichiometric effects of light/nutrient balance. Ecology 83, 619–627. https://doi.org/10.1890/0012-9658(2002)083[0619:rlihpd]2.0.co;2

Villar-Argaiz, M., Medina-Sánchez, J.M., Carrillo, P., 2002. Linking life history strategies and ontogeny in crustacean zooplankton: implications for homeostasis. Ecology 83, 1899–1914. https://doi.org/10.2307/3071773

Vrede, T., Dobberfuhl, D.R., Kooijman, S.A.L.M., Elser, J.J., 2004. Fundamental connections among organism C : N : P Stoichiometetry, macromolecular composition, and growth.

Ecology 85, 1217–1229. https://doi.org/10.1890/02-0249

Vrede T., Persson J., Aronsen G., 2002. The influence of food quality (P:C ratio) on RNA:DNA ratio and somatic growth rate of *Daphnia*. Limnol. Oceanogr. 47, 487–494.

Wong, E., Sastri, A.R., Lin, F., Hsieh, C., 2017. Modified FlowCAM procedure for quantifying size distribution of zooplankton with sample recycling capacity. PLoS One 12, 1–12.

Appendix A: Graphical illustration of artificial cohort incubation procedure and basic environmental conditions in the sampling areas

To better explain the procedure of our on board *in situ* artificial cohort incubation, we present a flow-chart to describe each methodological step in Figure A.1. We prepared three replicates of incubation for both naupilar (50-80 μm) and copepodite (100-150 μm) stages and incubated the two copepod life stages for 24 and 48 hours, respectively. The details of the experimental design are described in **2. Materials and methods** section in the main text.

Our sampling program focused on three areas: (1) the southern East China Sea (black dots); (2) the northern East China Sea (red dots); and (3) the Dongsha atoll (green dots) in the South China Sea (Fig. A.2). Detailed information on date, geographic coordinates and environmental conditions of each sampling and experiment, as well as primary and copepod production data are provided in Table A.1. The wide ranges of nutrient and chlorophyll *a* concentrations reflect the large gradient of trophic status in our study data.

Table A.1. Table of sampling dates latitude (°), longitude (°), weight-specific growth rate (GR; d^{-1}), temperature-standardized copepod production (CP; mg C m^{-3} d^{-1}), primary production (PP; mg C m^{-3} d^{-1}), and environmental conditions (xls file **TableA1_CPdatabase.xls**).

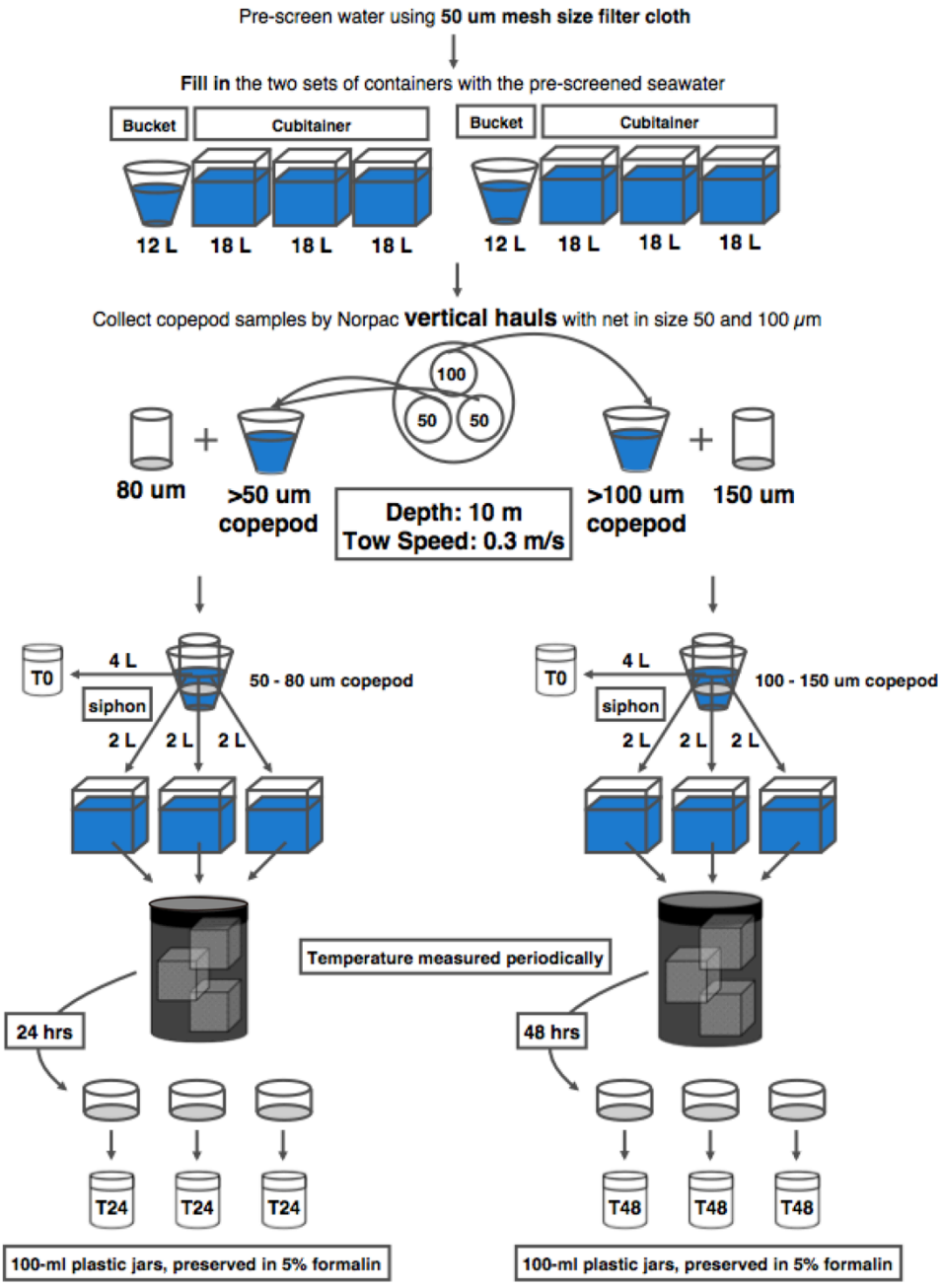

Figure. A.1. Procedure of *in situ* artificial cohort incubation experiment.

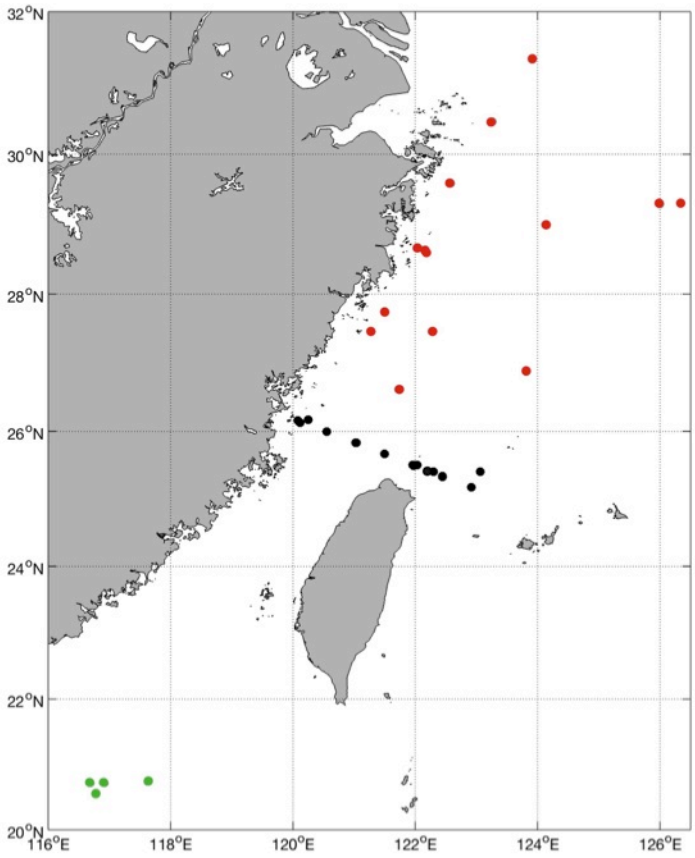

Figure A.2. Map of sampling area. Black symbols indicate sampling sites of the southern East China Sea transect; red symbols indicate sampling sites in the northern East China Sea; green symbols represent sampling sites around the Dongsha atoll.

Appendix B: Stoichiometry, growth rate and production of copepod juvenile stages

The quantile regressions showed complex relationship between copepod production (CP) and prey stoichiometry. The associations between CP and prey C:N and C:P ratios are not clear for low CP quantiles (quantile regressions were not statistically significant below 50 % quantiles; Fig. B.1), indicating that other factors influence low CP when nitrogen and phosphorus are not limiting. To further investigate the stoichiometry and life stages of copepod consumers and its possible link to production and growth rates, we measured the C:N and C:P ratios of plankton size fractions 50−104 μm (dominated by nauplii), and 104−200 μm (dominated by copepodites). The samples collected by the 50-μm mesh size Norpac net were processed through analytical sieves of 200-, 104-, and 50-μm mesh. C, N, P contents of the two target size fractions were measured following the same protocol as POM stoichiometry (see **2. Materials and Methods** section). Previous studies have found that C:N and C:P ratios vary with copepod life stages, due to their different energy allocation strategies. In general, the naupliar stages have lower C:P but higher C:N ratios than the copepodite stages (Villar-Argaiz et al., 2002). Results of our field analyses also show that copepodites have significantly lower C:N ratio than nauplii (Fig. B.2a). This suggests that copepodites require more N to attain stoichiometric balance. In contrast, nauplii have slightly lower and less variable N:P ratio than copepodites (Fig. B.2c), and C:P ratios do not differ significantly between naupliar and copepodite stages (Fig. B.2b). This indicates that nauplii may require phytoplankton with higher P relative to N and a more stable N:P ratio of their food. Some samples exhibited extremely high C:N or C:P ratios, which may be due to the influence of C-rich detritus when processing samples through analytical sieves. Nevertheless, we still observed this general stoichiometric pattern of nauplii and copepodites.

In most cases, copepodite production and biomass dominates the total community CP and zooplankton biomass (Fig. B.3 and B.4). The dominance of copepodites in CP and their apparent requirement for lower C:N in food may explain why phytoplankton C:N ratio plays a more important role than C:P ratio in influencing total CP (Fig. 1a and 1b).

Interestingly, though CP is only significantly correlated with POM C:N ratio, community GR is significantly correlated only with prey C:P ratio (Fig. B.5). This implies that P is a more important element to growth (Main et al., 1997). Copepod community mean growth rate is calculated as the biomass weighted-mean growth rate of all copepodite and nauplius groups $\mathrm{GR} = \frac{\sum B_i \mathrm{GR}_i}{\sum B_i}$. The community mean GR is not significantly correlated with POM C:N ratio ($y = -0.018\ x + 0.284$, $R^2 = 0.026$, $p = 0.242$; Fig. B.5a), but is significantly and negatively correlated with POM C:P ratio ($y = -9.298\times10^{-5}\ x + 0.203$, $R^2 = 0.117$, $p = 0.038$; Fig. B5b), although the trend is heavily influenced by the extremely high C:P ratio. The reason why CP is,

but GR is not, significantly correlated with prey C:N ratio is that sufficient N in prey is necessary for copepodite biomass production. We infer that total CP decreases with high prey C:N ratio because a high prey C:N ratio reduces the efficiency to maintain and produce proteinaceous body structures of copepods (Carrillo et al., 2001).

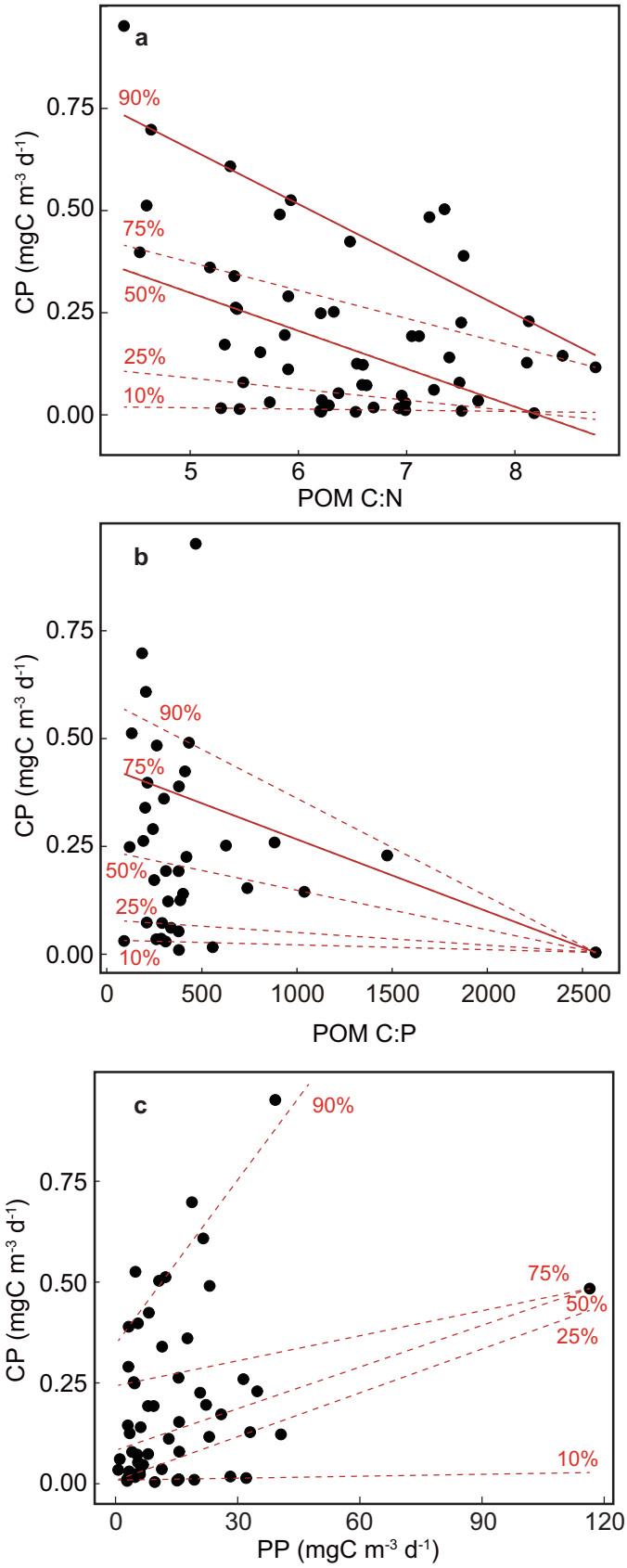

Figure B.1. Quantile regressions between copepod production (CP) versus POM (a) molar C:N, (b) C:P ratios, and (c) PP. The regressions of 10%, 25%, 50%, 75% and 90% quantile regressions are shown. Solid lines represent regressions with $p < 0.05$ and dotted lines represent regressions with $p \geq 0.05$.

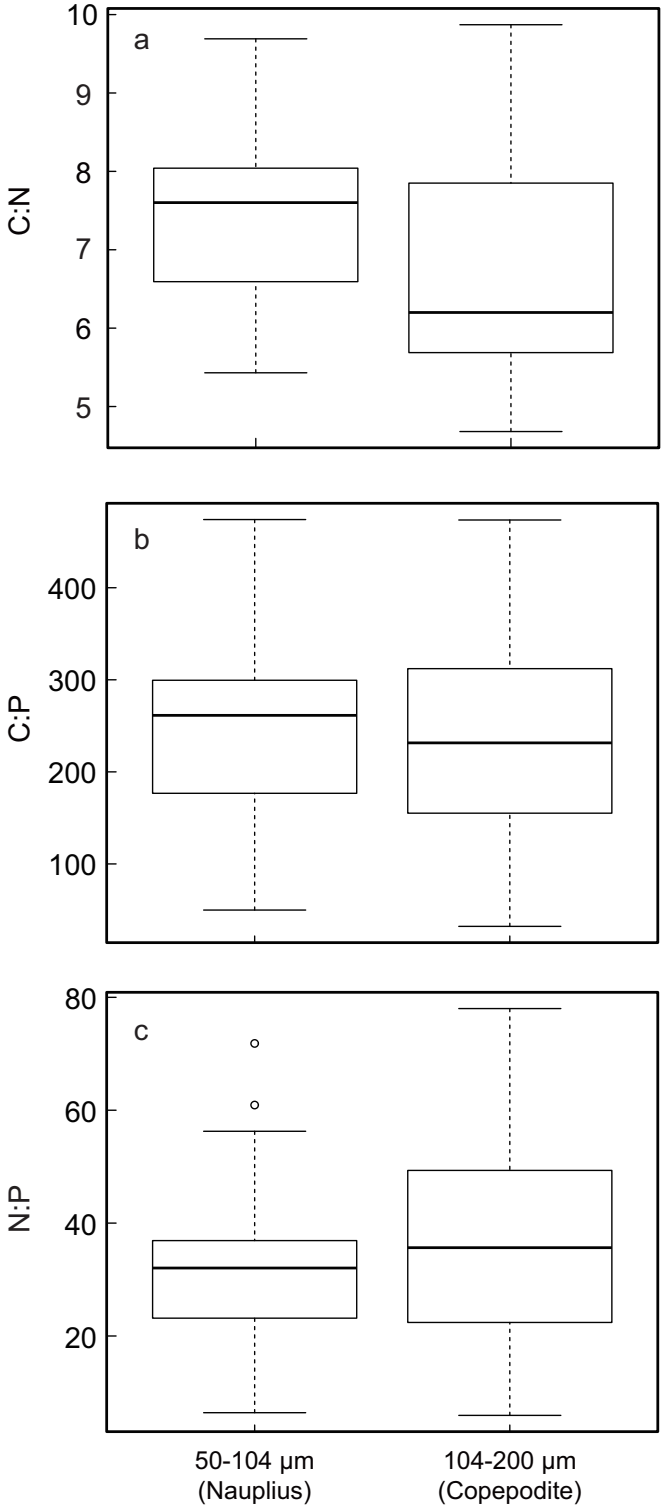

Figure B.2. C:N and C:P and N:P ratio of naupliar and copepodite stages. The mean C:N ratio (a) of naupliar stages is significantly greater than that of copepodite stages (t-test. $t = -2.914$, $p = 0.0046$). The mean C:P (b) and N:P (c) ratios of naupliar and copepodite stages are not significantly different (t-test. $t = -0.349$, $p = 0.729$; $t = 0.713$, $p = 0.479$).

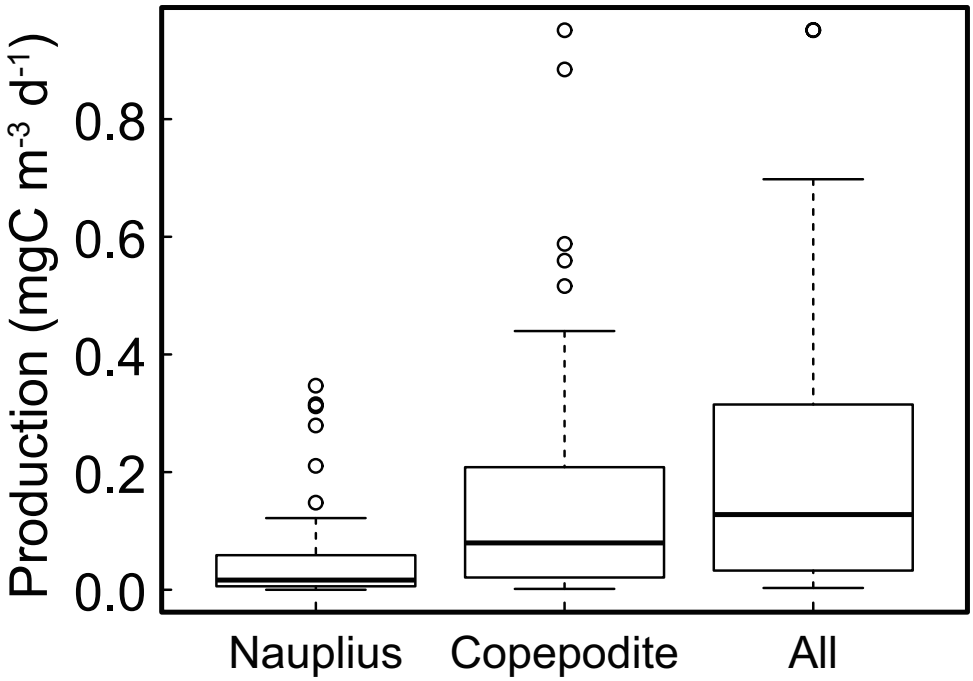

Figure B.3. Production of naupliar and copepodite stages, and the entire copepod community (All). Community copepod production (CP) is usually dominated by copepodites.

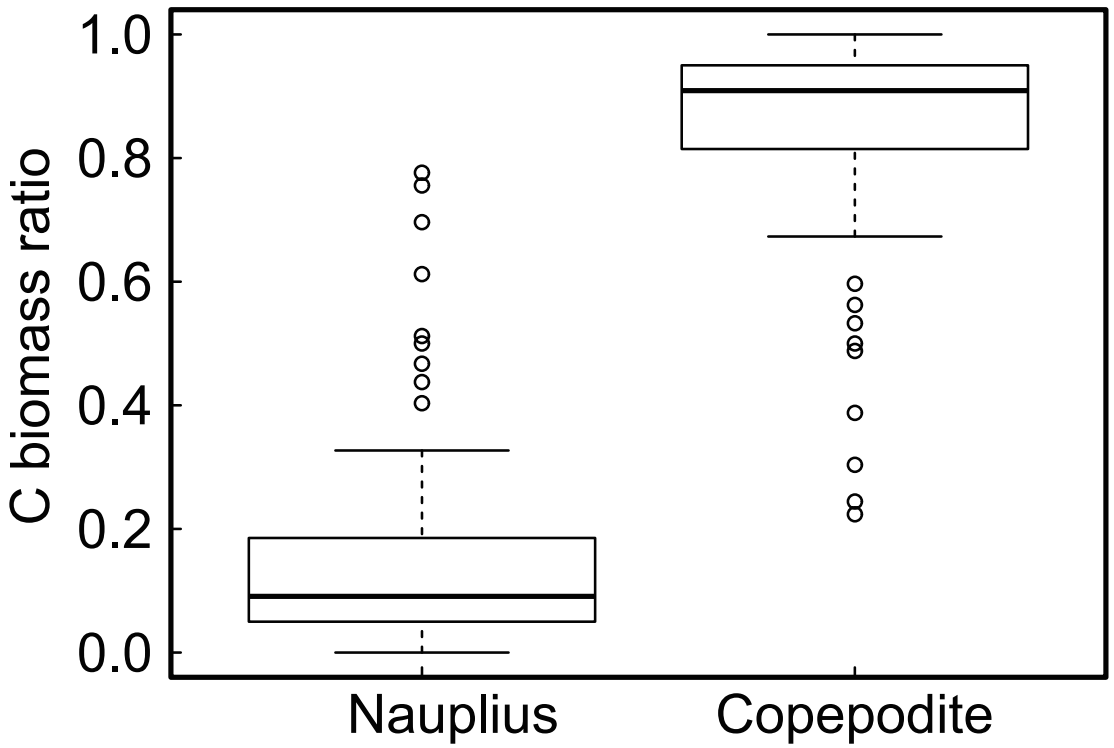

Figure B.4. Ratios of C mass of naupliar and copepodite stages to total copepod C biomass.

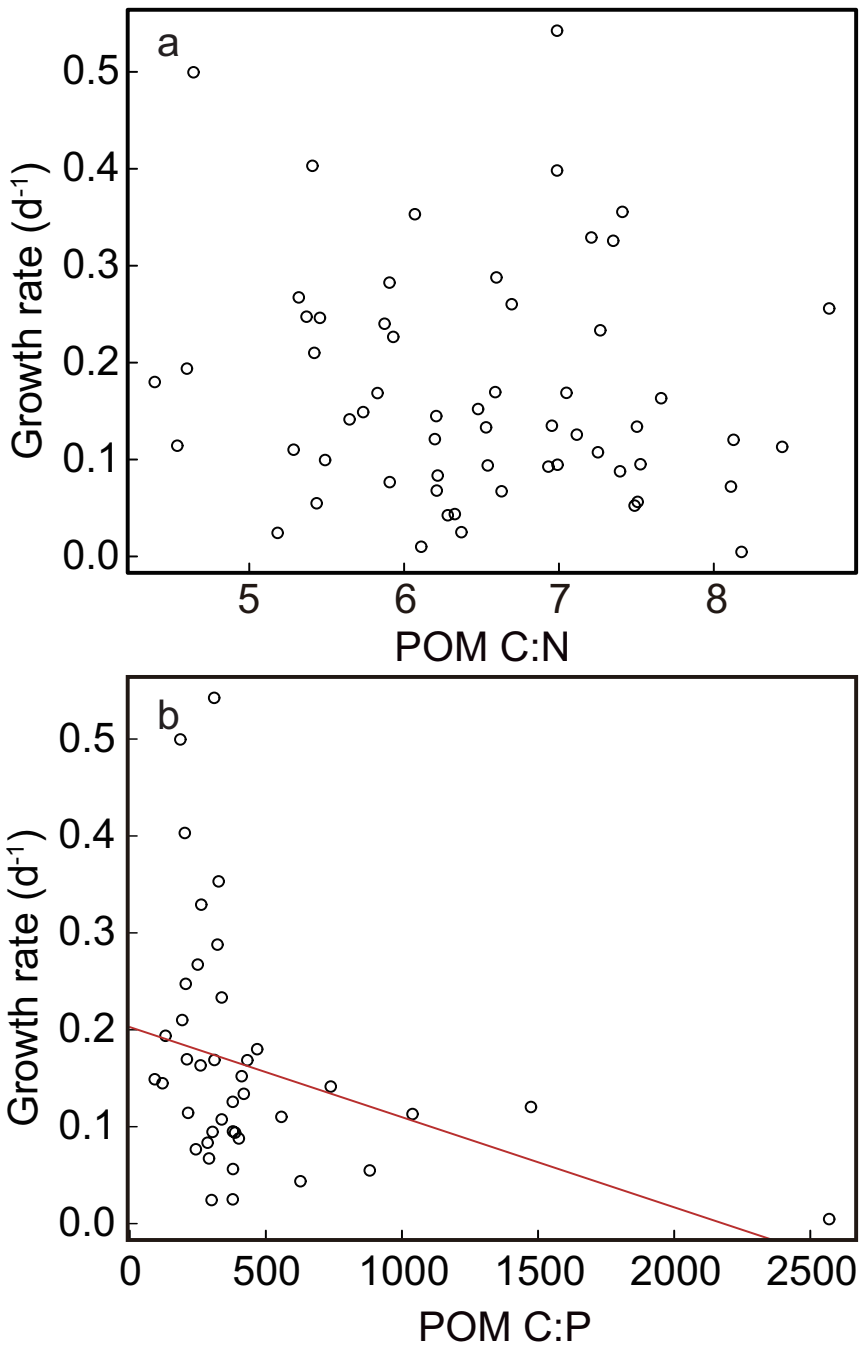

Figure B.5. Relationship between copepod community growth rate (GR) versus (a) POM C:N ratio and (b) POM C:P ratio. The solid red line represents the result of significant linear regression ($p < 0.05$).

References

Carrillo, P., Villar-Argaiz, M., Medina-Sánchez, J.M., 2001. Relationship between N : P ratio and growth rate during the life cycle of calanoid copepods: An *in situ* measurement. J. Plankton Res. 23, 537–547. https://doi.org/10.1093/plankt/23.5.537

Main, T.M., Dobberfuhl, D.R., Elser, J.J., 1997. N : P stoichiometry and ontogeny of crustacean zooplankton: A test of the growth rate hypothesis. Limnol. Oceanogr. 42, 1474–1478.

Villar-Argaiz, M., Medina-Sánchez, J.M., Carrillo, P., 2002. Linking life history strategies and ontogeny in crustacean zooplankton: implications for homeostasis. Ecology 83, 1899–1914. https://doi.org/10.2307/3071773

673
674
675
676
677
678
679
680
681
682
683
684
685
686
687
688
689
690
691
692
693
694
695
696
697
698
699
700
701
702
703
704
705
706
707
708
709
710
711
712
713
714
715
716
717
718
719
720
721
722
723
724
725
726
727
728

Appendix C: Phytoplankton and copepod compositions

The phytoplankton community was sampled using 20 L Go-Flo bottles. The procedures have been explained in García-Comas et al. (2016) and are briefly described here. From sea surface to the Chl-*a* maximum, 333 or 250 mL of seawater was sampled at 3 or 4 depths and was then thoroughly mixed (making up the total water volume of 1000 mL) to represent the phytoplankton community in the euphotic zone. The samples were preserved in 0.2% paraformaldehyde (nanophytoplankton, <50 μm) and 2% acidic Lugol's solution (microphytoplankton, 50−200 μm) and stored at 4 °C. Due to the low particle density, 100 mL of microphytoplankton sample were condensed by sedimentation for 24 hours to 3.6−4.5 mL. Nanophytoplankton samples were not concentrated before analysis. We subset 0.5−5 mL (nanophytoplankton) and 3.6−4.5 mL (concentrated microphytoplankton) samples for each run. The cells of phytoplankton were measured with the FlowCAM (Álvarez et al., 2014, 2011; Ide et al., 2008). Following the manufacturer's manual, the 10X objective was used with a 100 μm flow cell for nanophytoplankton and the 4X with a 300 μm flow cell for microphytoplankton. The phytoplankton images were captured and processed in autoimage mode. Phytoplankton images were thereafter manually checked, and detritus images were removed. Non-detritus particles captured by FlowCAM were further classified into 7 groups: Small (<5 μm phytoplankton), Medium (5−50 μm), Large (50−200 μm phytoplankton that are not diatom, dinoflagellate, ciliate, or cyanobacterium), Diatom (chain-forming and single diatom), Dino (shelled and naked dinoflagellate), Ciliate (tintinnid and other naked ciliate), and Cyano (filamentous cyanobacterium, mainly *Trichodesmium* (Chang et al., 2000)). We ran 3 replicates and 2 replicates, respectively, for nanophytoplankton and microphytoplankton, and took the average of the replicate runs.

The boxplots of phytoplankton biomass composition ratio (Fig. C.1a) showed that small phytoplankton, ciliates and *Trichodesmium* spp. are very low in biomass. Due to the detection limit and resolution of the FlowCAM, cells <5 μm were difficult to identify and their density was likely underestimated (Dashkova et al., 2017). Ciliates, especially naked ciliates, may suffer from shrinkage and biomass underestimation (Choi and Stoecker, 1989). The contribution of *Trichodesmium* to phytoplankton production is low (Chang et al., 2000), and is probably not a major dietary component for copepod. In addition, although *Trichodesmium* can be grazed by some harpacticoid species (Roman, 1978), a stable isotope study also revealed that *Trichodesmium* does not dominate the diet of copepods in nature (Eberl and Carpenter, 2007). Given the factors above, we did not include these three groups in the multivariate regression analysis.

The zooplankton community samples were collected with oblique net hauls using a 50-μm mesh Norpac plankton net and were preserved in sea water-buffered 10% formalin. We manually

counted copepodites and nauplii under a dissecting microscope to obtain the abundance of each group. Naupliar stages were the most abundant group and calanoids and cyclopoids dominated the copepodite community (Fig. C.1b). The other three groups were low in abundance and their contribution to CP is small. Thus, we mainly considered nauplii, and calanoid and cyclopoid copepodites abundance ratios in our multivariate regression model.

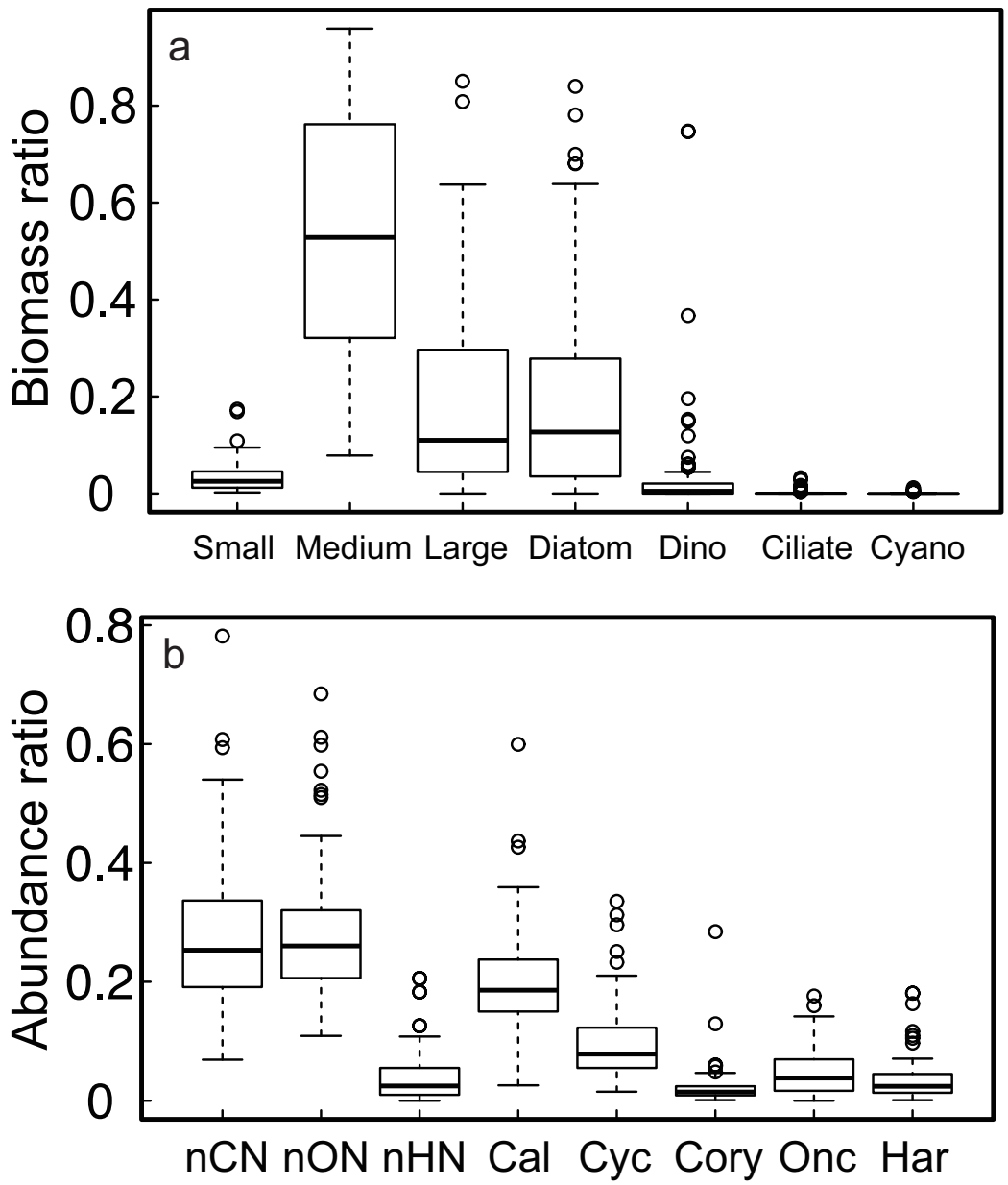

Figure C.1. Boxplots illustrating the phytoplankton biovolume (μm^3 mL^{-1}) ratio (a) and copepod composition based on the abundance (ind m^{-3}) ratio (b). In (a), *Small*, *Medium* and *Large* represents the phytoplankton of size range <5 μm, 5-50 μm, and 50-200 μm; *Dino* and *Cyano* indicates dinoflagellate and cyanobacteria, respectively. In (b), *nCN*, *nON*, and *nHN* represents the nauplii of calanoid, cyclopoid, and harpacticoid. *Cal*, *Cyc*, *Cory*, *Onc*, and *Har* represents the copepodites of calanoid, cyclopoid, corycaeid, oncaeid, and harpacticoid.

References

Álvarez, E., López-Urrutia, Á., Nogueira, E., Fraga, S., 2011. How to effectively sample the plankton size spectrum? A case study using FlowCAM. J. Plankton Res. 33, 1119–1133. https://doi.org/10.1093/plankt/fbr012

Álvarez, E., Moyano, M., López-Urrutia, Á., Nogueira, E., Scharek, R., 2014. Routine determination of plankton community composition and size structure: A comparison between FlowCAM and light microscopy. J. Plankton Res. 36, 170–184. https://doi.org/10.1093/plankt/fbt069

Chang, J., Chiang, K., Gong, G., 2000. Seasonal variation and cross-shelf distribution of the nitrogen-fixing cyanobacterium, *Trichodesmium*, in southern East China Sea. Cont. Shelf Res. 20, 479–492.

Choi, J.W., Stoecker, D.K., 1989. Effects of fixation on cell volume of marine planktonic protozoa. Appl. Environ. Microbiol. 55, 1761–1765. https://doi.org/0099-2240/89/071761-05$02.00/0

Dashkova, V., Malashenkov, D., Poulton, N., Vorobjev, I., Barteneva, N.S., 2017. Imaging flow cytometry for phytoplankton analysis. Methods 112, 188–200. https://doi.org/10.1016/j.ymeth.2016.05.007

Eberl, R., Carpenter, E.J., 2007. Association of the copepod Macrosetella gracilis with the cyanobacterium *Trichodesmium* spp. in the North Pacific Gyre. Mar. Ecol. Prog. Ser. 333, 205–212. https://doi.org/10.3354/meps333205

García-Comas, C., Sastri, A.R., Ye, L., Chang, C., Lin, F., Su, M., Gong, G., Hsieh, C., 2016. Prey size diversity hinders biomass trophic transfer and predator size diversity promotes it in planktonic communities. Proc. R. Soc. B Biol. Sci. 283, 1–8.

Ide, K., Takahashi, K., Kuwata, A., Nakamachi, M., Saito, H., 2008. A rapid analysis of copepod feeding using FlowCAM. J. Plankton Res. 30, 275–281. https://doi.org/10.1093/plankt/fbm108

Roman, M.R., 1978. Ingestion of the blue-green alga *Trichodesmium* by the harpacticoid copepod, *Marcrostella gracilis*. Limnol. Oceanogr. `23, 1245–1248.